01 Sep 1998

Low-Field Hopping among Randomly-Distributed Sites with Uncorrelated Energetic Disorder

Paul Ernest Parris

Missouri University of Science and Technology, parris@mst.edu

Low-field hopping among randomly-distributed sites with uncorrelated energetic disorder

P. E. Parris[a)]
Department of Physics, University of Missouri-Rolla, Rolla, Missouri 65409

(Received 4 September 1997; accepted 25 September 1997)

The low-field mobility μ of a small concentration of charge carriers hopping among a random distribution of transport sites is studied, as a function of the mean interparticle spacing ρ and the temperature T, for model systems having different site-energy distribution functions. For a uniform density of states our calculations show that the mobility obeys empirical scaling laws similar to those found in the theory of variable-range hopping. For a binary distribution of site energies we observe a crossover as a function of site density between trap-limited conduction and trap-mediated conduction. For a Gaussian density of states our results confirm the quadratic inverse temperature dependence of $\ln\mu$ found in Monte Carlo studies, although quantitative characterization of this dependence is found to depend sensitively on the degree of spatial disorder in ways that could impact the extraction of microscopic parameters from experimental data. © *1998 American Institute of Physics.* [S0021-9606(98)51301-3]

I. INTRODUCTION

Photoconduction in molecularly-doped polymers and organic molecular glasses occurs as a result of carriers hopping among randomly-distributed transport molecules that have been incorporated for this purpose into the organic binder.[1–3] Many of the specific features associated with charge transport in these materials have been attributed to the effects of spatial and energetic disorder; the former arising from the random placement and orientation of transport molecules, the latter from random variation in local electronic environments associated with the structural disorder. In recent years considerable experimental effort has gone into empirically characterizing photoconduction in these materials in terms of a disorder-based formalism introduced by Bässler and Borsenberger.[2–5] The disorder formalism itself is based upon intuition gained from extensive Monte Carlo simulations[3,4,6] of the so-called Gaussian disorder model (GDM). In the GDM, transport occurs on the sites of a regular lattice, site energies are drawn from a Gaussian site-energy distribution function, and nearest-neighbor hopping rates are exponentially modulated by additional Gaussian random variables intended to incorporate the effects of geometrical or spatial disorder.[4] The assumption of a Gaussian site-energy distribution has gained some recent support from experimental and theoretical evidence[7–20] linking the source of energetic disorder in these materials to Gaussian fluctuations in the electrostatic potential caused by permanent dipoles of host and dopant molecules.

Detailed theoretical studies of the dipolar model of disorder, however, indicate that the Gaussian nature of the density-of-states function is only approximate.[14,16,20] Moreover, in a number of recent experimental papers, additional transport molecules have been doped into the medium to clarify transport mechanisms associated with deep trapping levels.[21–24] For such materials, the traditional assumption of a unimodular Gaussian site-energy distribution function becomes more difficult to justify, and a sharpened understanding of the general dependence of hopping transport on the density-of-states function is required.

With the intention of addressing some of these questions, we present in this paper model calculations of the low-field mobility for charge carriers hopping in an energetically and spatially disordered medium. Unlike previous Monte Carlo studies associated with the Gaussian disorder model, our focus in the present study is on systems in which the spatial distribution of hopping sites is completely random, i.e., there is no underlying lattice, and each transport site is placed independently of the others, keeping the mean density n_0 of hopping sites fixed. We consider models in which the site energies ϵ_n are independently distributed random variables, ignoring in the present study any spatial correlations of the type that have been shown recently to affect the field dependence of the mobility.[15,17,18] Each of the three models studied below is characterized by a different site energy distribution function, or density of states (DOS), which we denote by $g(\epsilon)$. As a baseline, we first consider the simplest density-of-states function with a well-defined nonzero width, namely, a DOS which is uniform over some interval. We find that transport in this model displays a crossover between nearest-neighbor hopping and a single-particle form of variable range hopping, displaying the characteristic temperature dependent scaling associated with the latter. Next, we consider a binary distribution of site energies, as would be associated with a small concentration of sharply defined trapping centers, and observe a crossover as a function of site density between trap-limited and trap-mediated conduction. Finally, to make contact with the GDM, we consider a Gaussian density of states, comparing and contrasting our results with those obtained in the low-field limit of standard lattice simulations of that model. All calculations in the present study were performed using a computational approach originally developed to study transport on substitutionally-disordered

[a)]Electronic mail address: parris@umr.edu.

 0021-9606/98/108(1)/218/9/$15.00

lattices[25,26] that is particularly suited for calculating the drift mobility at very low fields, a regime that is often difficult to access in simulation. A review of the algorithm, first presented in Refs. 25 and 26, and its extension to the topologically disordered systems of the present study appears in the appendix. To aid comparison with the extensive simulations that have been performed within the Gaussian disorder model, we focus in the present study only on systems with hopping rates obeying an asymmetric detailed balance relation[27]

$$W_{nm}=\nu_0\exp\left[-\alpha r-\frac{\beta}{2}(\epsilon_n-\epsilon_m-|\epsilon_n-\epsilon_m|)\right], \tag{1}$$

in which W_{nm} denotes the hopping rate from a site m to site n separated by a distance r. In this expression, the parameter α governs the effective range of the hopping rate (it is equivalent to the factor 2γ found, e.g., in Ref. 4), $\beta=1/kT$ is the inverse temperature, and ν_0 is an overall attempt frequency.

II. UNIFORM DENSITY OF STATES

We begin by considering hopping among states in which the DOS function is uniform throughout some energy range, i.e., we take

$$g(\epsilon)=\begin{cases} W^{-1} & W\geqslant\epsilon\geqslant 0 \\ 0 & \text{otherwise} \end{cases}, \tag{2}$$

where W is a measure of the width of the distribution. In Fig. 1, calculations of the mobility are presented as a function of the mean interparticle spacing $\rho=n_0^{-1/3}$, scaled by the parameter α which governs the exponential falloff of the rates. The different curves in this figure correspond to calculations performed for different energy widths at fixed temperature, or equivalently, to fixed energy widths at different temperatures. In the figure they are parameterized by the dimensionless quantity $\hat{W}=\beta W$, the inverse of which gives the approximate equilibrium fraction of the total number of sites in the system which are populated by charge carriers. Calculated data points are explicitly included only for the topmost curve, for which there is no energetic disorder ($\hat{W}=0$). The accompanying curve runs smoothly through all the data points, which show very little statistical fluctuation. This behavior is typical of all the calculations that we have performed. Hence, for the remaining curves in this and in most of the later figures we have, for the sake of legibility, included only the accompanying smooth curves.

We note the strong, approximately exponential, falloff with mean interparticle spacing, which is one of the signatures of a hopping process. At low values of the mean interparticle spacing, a carrier at any given site typically has several comparably probable sites to choose from as it migrates through the system. At higher values of $\alpha\rho$, for nearly degenerate energies $\hat{W}\simeq 0$, the system exhibits nearest-neighbor hopping, with conduction taking place through a percolating critical path of sites; the hopping rate from any given site being exponentially dominated by the single site to which it is closest. At higher values of $\hat{W}$, hopping does not necessarily occur to the site which is closest in space, since such sites may typically be of very different energy. Thus, in this latter regime particles undergo hops of variable range.[28]

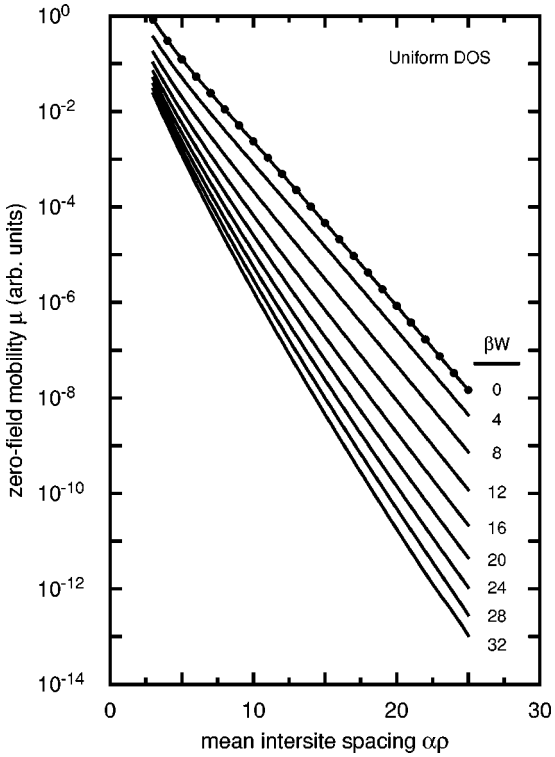

FIG. 1. Computed mobility μ as a function of the dimensionless mean interparticle spacing $\alpha\rho=\alpha n_0^{-1/3}$, for a system with a uniform density of states of width W. Top curve corresponds to randomly-placed degenerate hopping sites ($W=0$). Remaining curves correspond to systems with increasing energetic disorder, as determined by the dimensionless parameter $\hat{W}=\beta W$.

Traditionally, the term variable-range-hopping is associated with a small concentration of carriers hopping among localized states within a narrow region of order kT above a filled Fermi sea of localized states. The filled lower energy states provide a lower cutoff in the states accessible to a particle moving through the medium. The uniform density of states (2) mimics this behavior, where, with $\epsilon_f=0$, the quantity $n_0W^{-1}\simeq N(\epsilon_f)$ can be associated with the energetic density of states per unit volume at the Fermi energy. Thus, we might expect that under appropriate limits this model should exhibit the well-known scaling behavior associated with Mott's picture of variable-range hopping.[29–31] A number of different scaling arguments suggest that for a uniform energy distribution the mobility in the variable-range hopping regime should take the form[29–31]

$$\mu\sim\exp[-A(\alpha^3\rho^3W/kT)^{1/4}], \tag{3}$$

where A is a universal constant. In Fig. 2, to study the scaling behavior of the present model, the data of Fig. 1 have been replotted as a function of the dimensionless parameter $(\alpha^3\rho^3\beta W)^{1/4}$. The coalescence of the different curves appearing in Fig. 1 onto a single universal curve (represented

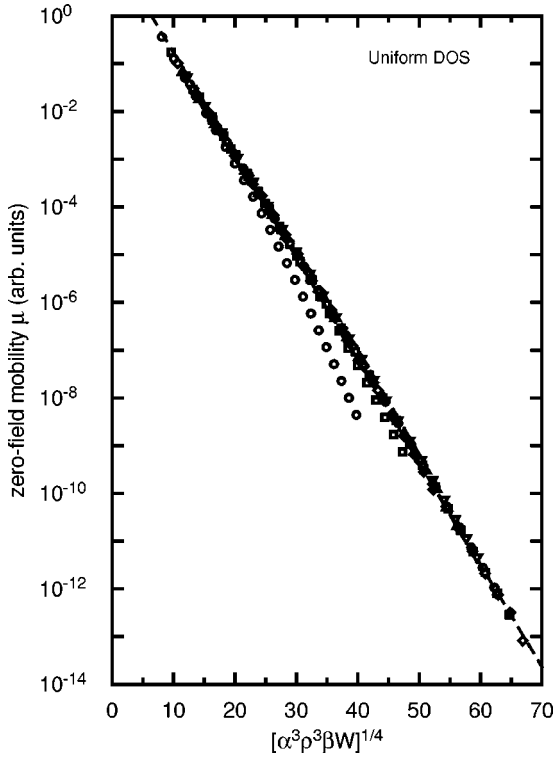

FIG. 2. Data from the bottom eight curves of Fig. 1 replotted as a function of the dimensionless scaling parameter $(\alpha^3\rho^3\beta W)^{1/4}$. Open circles and squares correspond, respectively, to $\beta W=4$ and 8. Dashed curve corresponds to the function $\mu \propto \exp[-A(\alpha^3\rho^3\beta W)^{1/4}]$, with $A=0.494$.

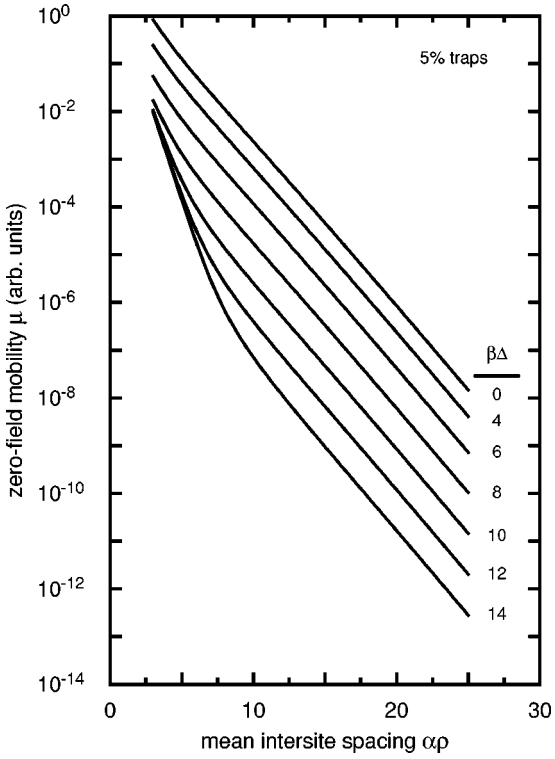

FIG. 3. Mobility μ for a system with a 5% concentration of traps of depth Δ as a function of $\alpha\rho=\alpha n_0^{-1/3}$.

by the dashed straight line) extending over nearly twelve orders of magnitude is in excellent agreement with the scaling predictions of Eq. (3), and confirms the soundness of the basic computational approach as applied to the present class of models. The small systematic deviation from the straight line exhibited by two of the data series (viz., those with open circles and open squares) is sensible, insofar as these correspond to curves with the lowest energy width, or equivalently, the highest temperature (for these curves $\hat{W}$ is equal to 4 and 8, respectively; note that it is impossible to include the data for $\hat{W}=0$ on such a plot, since it would reduce the entire horizontal axis to a single point). As ρ is increased, these two data series are seen to move off the universal curve associated with variable-range hopping as they move into the regime of nearest-neighbor hopping. We anticipate that, due to the upper cutoff on the density of states in this model, any series with fixed $\hat{W}$ will eventually move off of the universal curve at sufficiently large values of the mean interparticle separation.

III. BINARY DENSITY OF STATES

We next consider a model in which the DOS function, although it does have a sharp upper and lower cutoff, does not have states with energies *continuously* distributed over any particular energy range. Specifically, we consider a dichotomous or binary DOS function of the form

$$g(\epsilon)=p\,\delta(\epsilon)+(1-p)\,\delta(\epsilon-\Delta) \tag{4}$$

which describes two types of sites: lower energy ''traps'' $(\epsilon=0)$ which exist in relative concentration p and higher energy sites $(\epsilon=\Delta)$ in relative concentration $(1-p)$. The dimensionless quantity $\hat{\Delta}=\beta\Delta$ is a measure of the trap depth. At sufficiently low temperatures (large $\hat{\Delta}$) and for small trap concentrations p, we might expect to find that conduction in this system is *trap-limited* in the sense that carriers will spend a large amount of time in traps waiting to be promoted to the more dense array of higher energy states among which transport more readily occurs. For any value of p, however, it is possible to reduce the mean interparticle separation sufficiently that thermally-activated hops out of the lower energy traps will begin to be shorted out by direct hops to other traps, which are typically farther away, but for which there is no energy mismatch to impede the process. Thus there will be a narrow range in which variable-range hops will occur as a result of the crossover between trap-limited conduction and direct *trap-mediated* conduction. In Figs. 3–5, we present calculations for systems of this type with three different trap concentrations, $p=0.05$, 0.1, and 0.2, respectively.

Again, the different curves in each figure can be interpreted either as different energies at fixed temperature, or different temperatures at fixed energy, with the relevant dimensionless parameter being the dimensionless trap depth $\hat{\Delta}=\beta\Delta$. In these curves we note the characteristic features described above, with the lowest curves (lowest temperature/deepest traps) showing a distinct crossover between trap-mediated conduction at small interparticle separations and

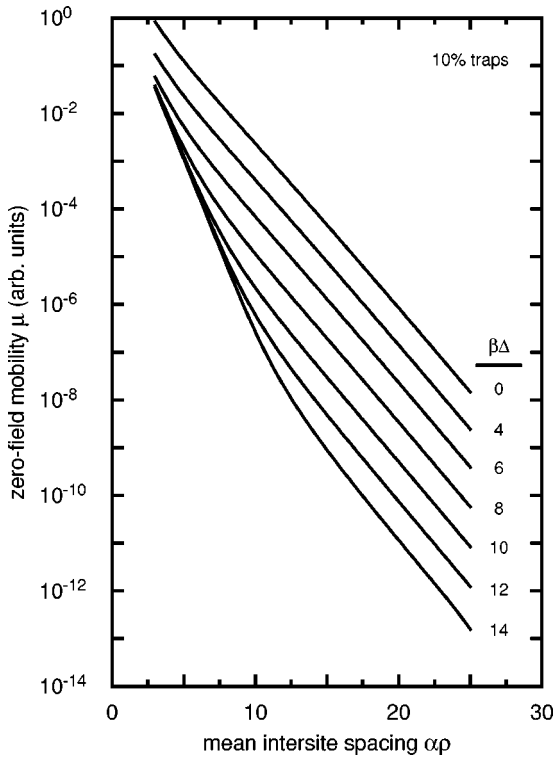

FIG. 4. Mobility μ for a system with a 10% concentration of traps of depth Δ as a function of $\alpha\rho=\alpha n_0^{-1/3}$.

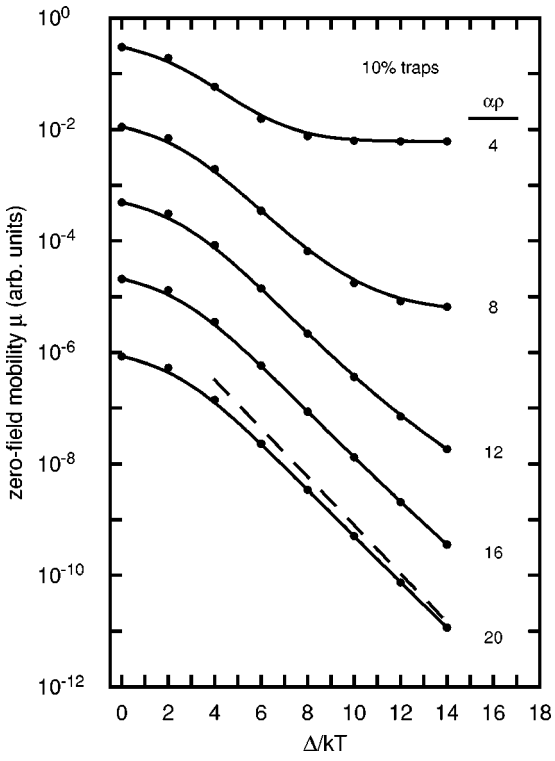

FIG. 6. Mobility μ as a function of $\hat{\Delta}=\Delta/kT$ for a system with a 10% concentration of traps.

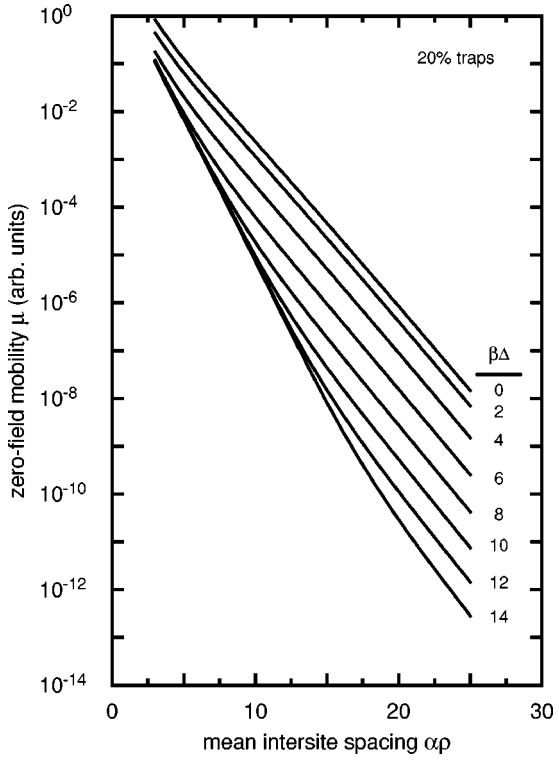

FIG. 5. Mobility μ for a system with a 20% concentration of traps of depth Δ as a function of $\alpha\rho=\alpha n_0^{-1/3}$.

trap-limited conduction at larger ones. In the trap-mediated regime the falloff with interparticle separation is steeper, since it is determined by the mean intertrap spacing $\rho_t=(pn_0)^{-1/3}=p^{-1/3}\rho$ which is larger by a factor of $p^{-1/3}$ than the mean interparticle spacing. This crossover can also be seen if we plot the mobility as a function of the trap depth $\hat{\Delta}$, for fixed values of the mean interparticle separation. In Fig. 6 we show such a plot for a trap concentration $p=0.1$, and several values of $\alpha\rho$ as indicated. For large values of $\alpha\rho$, and sufficiently large values of $\hat{\Delta}$, transport is trap limited, as discussed above, and the mobility shows a nearly Arrhenius temperature dependence. The dashed line in this figure represents the function $A\exp(-\Delta/kT)$, showing that the limiting slope of an Arrhenius plot at large interparticle separation is just the trap depth Δ. At smaller interparticle separations (i.e., smaller values of $\alpha\rho$), transport is shorted out by direct trap-to-trap transfer, which is not activated. This explains the flattening of the upper curves with increasing values of $\hat{\Delta}$. At all separations, when $\hat{\Delta}$ is very small, nearest-neighbor hopping occurs, and the mobility becomes independent of $\hat{\Delta}$. It is this effect that causes the flattening of each curve in the neighborhood of $\hat{\Delta}=0$.

IV. GAUSSIAN DENSITY OF STATES

Finally, we consider a Gaussian DOS function

$$g(\epsilon)=\frac{e^{-\epsilon^2/2\sigma^2}}{\sqrt{2\pi\sigma^2}}, \tag{5}$$

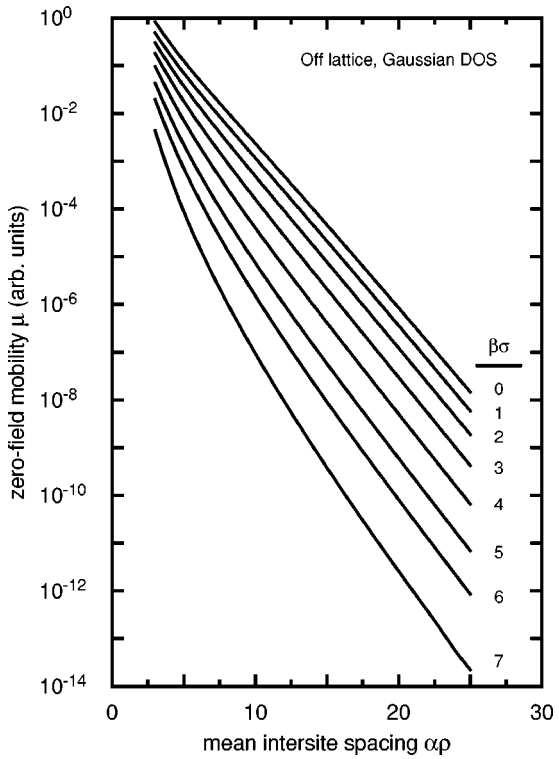

FIG. 7. Mobility μ for a system with a Gaussian density of states of width σ as a function of $\alpha\rho=\alpha n_0^{-1/3}$.

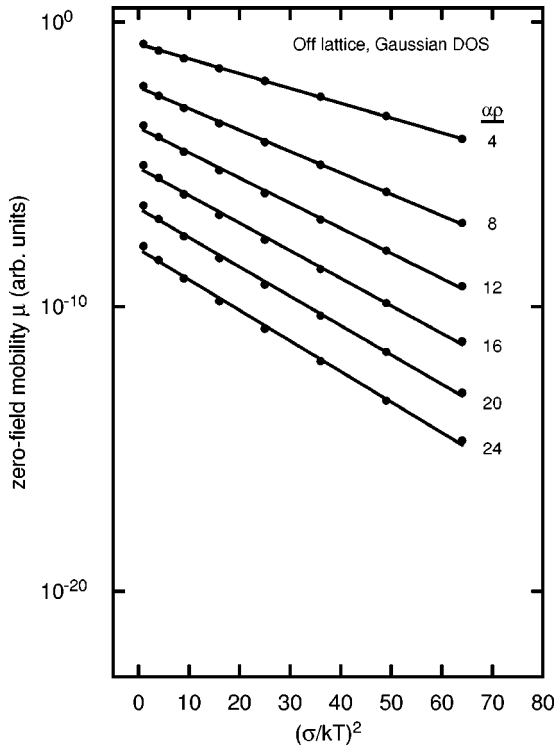

FIG. 8. Mobility μ as a function of the dimensionless parameter $\hat{\sigma}^2=(\sigma/kT)^2$ for a system with a Gaussian density of states of width σ, parametric in the mean interparticle spacing $\alpha\rho$. Transport sites are randomly placed. Computed data are represented by filled circles, straight lines are numerical fits.

of energetic width σ. This distribution function, unlike those discussed in Secs. II and III, does not have a sharp upper or lower cutoff. Indeed, the present model represents a variation of the Gaussian disorder model of Bässler *et al.*, in which transport sites are randomly distributed in space, rather than being located on a lattice[3,4]. In Fig. 7, calculations of the mobility are presented for particles moving in a Gaussian DOS as a function of the mean interparticle spacing $\rho=n_0^{-1/3}$, again scaled by the parameter α governing the exponential falloff of the rates. As in the previous example, different curves correspond to different energies at fixed temperature, or to fixed energies at different temperatures, parameterized now by the dimensionless width $\hat{\sigma}=\sigma/kT$.

Again we note a strong falloff with mean interparticle spacing. The curvature seen in those curves with the greatest amount of energetic disorder (or lowest temperatures) appears similar to the crossover behavior seen in the binary distribution. In the present circumstance, however, there is a continuous tail of lower energy states in the distribution. Thus, at low temperatures (large $\hat{\sigma}$) and small interparticle spacing, hopping predominately occurs among those states deep in the tail of the Gaussian distribution. As the mean interparticle spacing increases, so does the spacing between these lower energy sites, and more hops occur to states higher in energy but closer in space. In this way an ever increasing fraction of the total density of states becomes important as the spacing between particles increases. Thus there is a continuous change in the states of importance to transport with changing site density, temperature, and energetic disorder.

With a Gaussian density of states, the kind of analysis applied to deduce the scaling behavior for variable range hopping becomes analytically intractable.[32] Bässler and coworkers have performed extensive simulations to investigate the field dependence of the mobility for carriers moving through a Gaussian density of states.[3–5] On the basis of these simulations, it has been suggested that the extrapolated zero-field mobility is consistent with a function of the form

$$\mu=\mu_0\exp(-A\hat{\sigma}^2), \tag{6}$$

where μ_0 is a prefactor that is presumed to be independent of temperature (and also, therefore, of the energetic disorder), and $A=4/9$. In Fig. 8, we present our calculations of mobility as a function of the parameter $\hat{\sigma}^2=(\sigma/kT)^2$, for systems with different concentrations of transport sites (i.e., parametric in the mean interparticle spacing $\alpha\rho$). Actual data are indicated as filled circles, straight lines represent linear fits to the data.

It is clear from the figure that the quadratic inverse temperature dependences observed in numerical studies of the GDM are consistent with our results. On the other hand, our study indicates that the actual slope, $|\partial\ln\mu/\partial\hat{\sigma}^2|$, appearing in these plots is a slowly varying function of the mean interparticle separation ρ and is significantly different in magnitude than the ρ-independent value 4/9 advocated in the disorder formalism. To aid comparison with previous Monte Carlo studies of the GDM, we have performed similar calculations

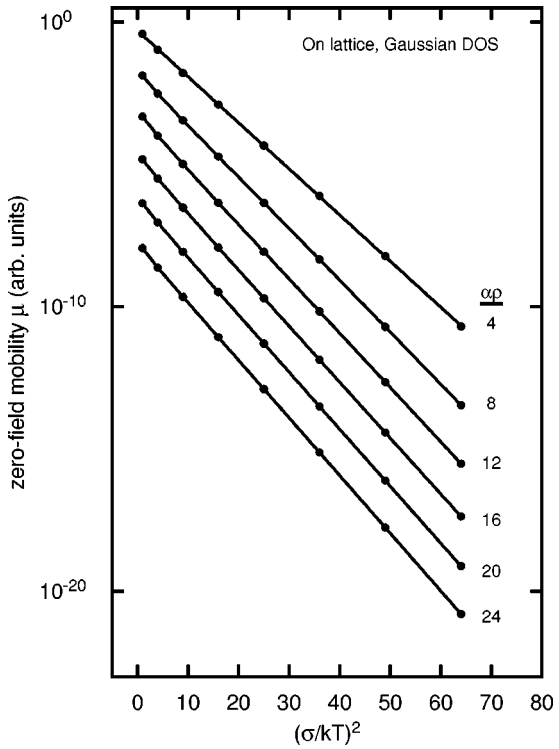

FIG. 9. Mobility μ as a function of the dimensionless parameter $\hat{\sigma}^2=(\sigma/kT)^2$ for a system with a Gaussian density of states of width σ, parametric in the mean interparticle spacing $\alpha\rho$. Transport sites are located on an ordered and filled lattice with unit cell spacing ρ. Computed data are represented by filled circles, straight lines are numerical fits.

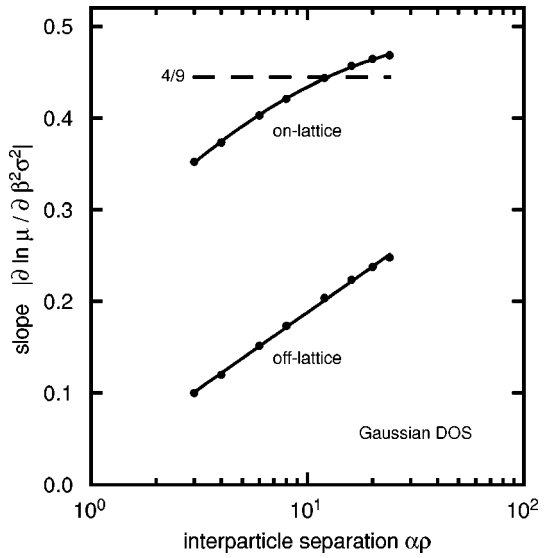

FIG. 10. The slope $|\partial \ln\mu/\partial\beta^2\sigma^2|$ of the data presented in Figs. 8 and 9 as a function of the mean interparticle spacing. Data labeled ''off-lattice'' are taken from the fits of Fig. 8, data labeled ''on-lattice'' are from Fig. 9. Horizontal dashed line shows the slope $A=4/9$ used in the disorder formalism of Ref. 4.

with no spatial disorder, i.e., with all sites placed on an ordered and filled lattice, as in the studies of Bässler *et al.*[3,4] with vanishing off-diagonal disorder parameter Σ. Our results, presented in Fig. 9, appear similar to those in Fig. 8, except the temperature dependence in the lattice calculation is stronger (i.e., the slope is steeper) for a given value of the mean interparticle spacing (which is now just equal to the unit cell distance), and variation of the slope $A=|\partial \ln\mu/\partial\hat{\sigma}^2|$ with ρ is somewhat weaker than when transport sites are distributed randomly.

In Fig. 10 we present, in the data points labeled ''off-lattice,'' a linear-log plot of the slopes obtained in the fits of Fig. 8, as a function of $\alpha\rho$. The straight line running through the data is a fit to a function of the form $|\partial \ln\mu/\partial\hat{\sigma}^2| = a+b\ln\alpha\rho$, with $a=0.0214$ and $b=0.0723$. In the data labeled ''on-lattice'' in the same figure we show the slopes obtained in fits to the lattice calculation of Fig. 9. The smooth curve running through these latter data is the function $|\partial \ln\mu/\partial\hat{\sigma}^2|=a+b\ln\alpha\rho+c\ln^2\alpha\rho$ with $a=0.242$, $b=0.114$, and $c=-1.32\times10^{-2}$. The universal slope $A=4/9$ used in the disorder formalism of Bässler and Borsenberger is indicated by a horizontal dashed line; it appears to be numerically exact for a filled lattice with mean interparticle spacing $\alpha\rho=12$, and is within 20% of the slope obtained in the lattice calculation for all values of $\alpha\rho$ considered. Thus, our calculations for transport on a filled lattice are in reasonable, although not exact, agreement with the results of previous Monte Carlo calculations, while our results for randomly-distributed hopping sites disagree significantly with the magnitude of the slope $|\partial \ln\mu/\partial\hat{\sigma}^2|$, in some cases by more than a factor of 4.

Some of the difference between results of the present study of random systems, as represented by Fig. 8, and those of earlier workers is due to the different manner in which we have treated spatial disorder. In the data of Fig. 8 and the lower curve of Fig. 10, spatial disorder arises entirely from the random placement of particles in the system. Reducing the concentration of sites increases the magnitude of fluctuations relative to the length scale associated with the hopping rates. In the studies of Bässler and co-workers,[3,4] spatial or ''off-diagonal'' disorder is treated quite differently; all hopping sites are actually arranged on an ordered lattice, but hopping rates connecting them are exponentially modulated through a set of Gaussian variables characterized by a width Σ. Of course in the upper curve of Fig. 10 there is no spatial disorder at all, since all sites lie on an ordered, filled lattice. It is tempting to speculate that the two curves of that figure provide upper and lower bounds for the variation in slope that can arise as a result of density fluctuations in the medium. Thus, for example, the data for a model in which sites occur on a lattice of edge length a with a partial filling factor c and mean interparticle spacing $\rho=c^{-1/3}a$ might be expected to lie somewhere between the two curves of Fig. 10. In fact, the family of such curves, parameterized by the filling fraction c, should move smoothly from the top curve of Fig. 10, which is the representative member of that family with $c=1$, to the bottom curve, which can be viewed as the limiting member in which $c\to0$, but with a going to zero in such a way that the mean interparticle spacing $\rho=c^{-1/3}a$ approaches a constant. The field dependence of a model of this sort has been considered by Bässler and co-workers, who

concluded that $A=4/9$ is a reasonable estimate for the slope of the zero-field mobility for all values of c that they considered.[5]

It is important to point out, however, that the zero-field mobility obtained from previous Monte Carlo simulations has been almost universally obtained as an extrapolation to zero field ($E=0$) from a plot of $\ln\mu$ vs $\sqrt{E}$, from a region at very high fields where they are approximately proportional (i.e., where the mobility obeys an approximate ''Poole-Frenkel'' behavior[33,34]). Our analysis and calculational approach, by contrast, is sensitive to the true limiting value of the mobility as $E\rightarrow 0$. Of course, in many experiments this difference is unimportant because extrapolated mobilities agree with the actual value at zero field (since Poole-Frenkel behavior obtains down to the lowest fields measured).

V. SUMMARY

We have numerically explored the dependence of the zero-field mobility on the functional form of the energetic density of states characterizing the manifold of transport sites. Our results for a uniform density of states obey well-known scaling relations associated with variable-range hopping, and display a crossover to nearest-neighbor hopping at large intersite separations. Related, but different crossover behaviors occur as a function of mean interparticle separation for other density-of-state functions. Our analysis has identified characteristic behavior associated with trap-limited and trap-mediated conduction for a system with a binary density of states. We have verified, using an independent treatment of off-diagonal disorder, the quadratic inverse temperature dependence associated with transport in an uncorrelated Gaussian distribution of site energies; however, our analysis indicates an intrinsic concentration dependence to the slope of $\ln\mu$ when plotted as a function of the square of the inverse temperature. Moreover, the magnitude and specific concentration dependence of this slope appear to depend in an essential manner on the way in which off-diagonal or spatial disorder is treated.

For transport on an ordered lattice, we find satisfactory agreement with the magnitude $|\partial\ln\mu/\partial\hat{\sigma}^2|\sim 4/9$ deduced in previous Monte Carlo studies; but we find a substantial reduction from this value when transport sites are distributed at random. The degree to which the treatment of spatial disorder adopted in the present study is more or less realistic than that assumed in previous studies is difficult to quantify. The present treatment benefits by being based upon a well-defined physical model, i.e., point particles distributed at random, with fluctuations in hopping rates arising simply from the fluctuation in interparticle distances. On the other hand, our use of point particles to locate transport sites ignores excluded volume effects, and allows for the possibility of two or more transport sites located at arbitrarily close distances from one another. This latter possibility is, in a sense, avoided when the particles are located on a lattice, but it is not clear that a random exponential modulation of the hopping rates does not mimic this effect; at any rate it means that at short distances the distance dependent part of the exponential hopping rate reduces to unity, making it entirely dependent upon energetic mismatch.

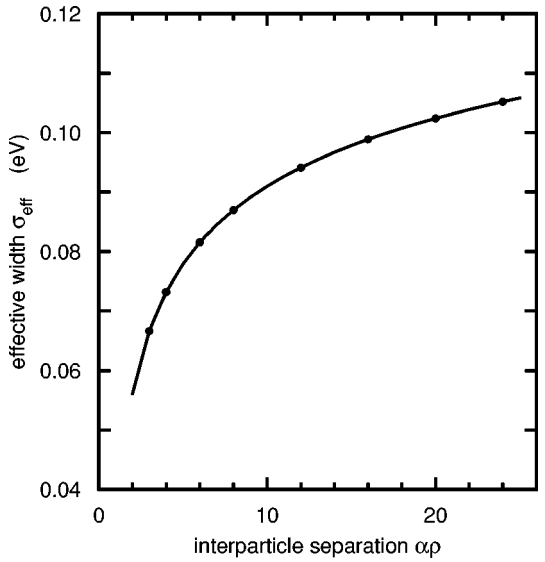

FIG. 11. Effective width $\sigma_{\rm eff}$ of the density of states deduced from the data of Fig. 8, assuming an actual width $\sigma=0.14$ eV and using Eq. (6) with $A=4/9$ to deduce $\sigma_{\rm eff}$. Data are plotted as a function of the mean interparticle spacing $\alpha\rho$, showing an artificial concentration dependence to the density of states arising from the fitting procedure.

It is interesting to note, however, that if the random model of off-diagonal disorder used in the present study is, in fact, a closer representation of the situation that occurs in real molecularly-doped organic solids, then an analysis of data performed assuming Eq. (6) with a concentration independent value $A=4/9$ could lead to incorrectly inferred values of the parameter σ, and to an incorrect dependence of the activation energy on transport site concentration. For example, suppose we replotted the curves in Fig. 8 simply as a function of β^2, keeping the actual value of σ fixed at one value, say 0.14 eV. The methods of the disorder formalism could then be applied to fit these data to Eq. (6) with $A=4/9$, thereby obtaining an effective value $\sigma_{\rm eff}=\frac{3}{2}\sqrt{|\partial\ln\mu/\partial\beta^2|}$ as a fitting parameter. This would, of course, correspond to the width that would be deduced using current methods of experimental data analysis, provided the extrapolated zero-field mobility is essentially the same as the true zero-field mobility calculated here. The result of such an exercise (which amounts to a simple transformation of the data in Fig. 10 labeled ''off-lattice''), is shown in Fig. 11. Thus, under this procedure one would deduce an erroneous increase in the width of the transport site manifold with interparticle separation. Similarly, in a situation in which the actual width of the density of states decreases with decreasing concentration (as is predicted, e.g., in various versions of the dipole disorder model[11,16,17]), the effect described above would be to partially or completely mask the concentration dependence resulting from increasing dipole densities.

It is tempting to argue, on the basis of our earlier statements indicating the importance of non-nearest neighbor hops, that the apparent increase observed in Fig. 11 is simply

a reflection of increasing participation in the transport process of a larger and larger fraction of the full density of states with increasing site separation, i.e., it basically results from variable range hopping as discussed in Sec. II. Thus, at small values of $\alpha\rho$, hops reflecting the full width of the density of states are rare, since a site has many neighbors of different energy in its immediate neighborhood to choose from. At larger separations the choice is reduced, and the quickest hop may indeed be to the site closest in space, even if it has very different energy. This explains the increasing slope in Fig. 8 with increasing values of $\alpha\rho$. Arguments of this sort, addressing the *experimentally observed* increase of σ with increasing ρ have been given previously in the context of an analytical study of hopping transport in a Gaussian density of states by Dunlap and Kenkre.[32] The extent to which these kind of variable-range-hopping considerations gain or lose importance in the presence of site-energy correlations, as arise in the dipolar disorder models of recent study, remains an important open question.

ACKNOWLEDGMENTS

This work was supported by the NSF under Grant No. DMR96-14849, and through the University of Missouri Research Board. The author acknowledges valuable discussions with B.D. Bookout, D.H. Dunlap, V.M.Kenkre, S.A. Novikov, and P.M. Borsenberger.

APPENDIX: COMPUTATIONAL METHOD

In this Appendix we describe the numerical approach used to compute the zero-field mobilities presented in Secs. II–IV. The computational problem is to obtain transport coefficients for charge carriers which hop among a random array of transport sites having random site energies ε_n, with transport sites in bulk concentration n_0, and carriers occupying the sites in fractional site concentration x. Our approach is essentially the same as that developed for energetically disordered lattices in Refs. 25 and 26. We first conceptually partition the actual disordered solid of interest into d-dimensional cubic regions of edge length L. Each such cube (or block) contains a random configuration of hopping sites, with site energies chosen from a particular density of states function $g(\epsilon)$. With the ith cube, which is assumed to typically contain a large number $N_i \simeq n_0 L^d \gg 1$ of sites, we associate a local conductance tensor γ_i. This conductance governs the current flow through that cube in response to electrical potential gradients imposed across its faces; it depends on the local carrier concentration x_i in that cube, and the Cartesian components of the local diffusion tensor D_i associated with carriers in that region.

We now map the original disordered system, conceptually decomposed as above, onto a new topologically-ordered lattice of lattice spacing L. The new system is intended to have the same bulk conductivity as the original. Provided that the edge length L of the lattice is large compared to the mean interparticle spacing *and* to the distance associated with a typical hop, this can be achieved by identifying the nearest-neighbor bonds coming out of the positive axis at each new lattice point i with the corresponding Cartesian components γ_i^ν of the associated block conductance tensor. For sufficiently large cubes, these conductances will be independent of one another, and can be taken as independently distributed random variables. Thus, we now have a lattice problem characterized by a bond conductance distribution function $\rho_L(\gamma_i)$.

This formal renormalization procedure outlined above could be repeated on a larger length scale in an attempt to find a fixed point.[35,36] In practice, the distribution $\rho_L(\gamma_i)$ of block conductances obtained after a single decimation of the disordered system is smoother and more narrow than that of the microscopic conductances (i.e., rates) connecting individual sites in the original system. Exploiting this natural smoothing of the distribution function, we employ the ideas of effective medium theory on this larger length scale. Within the well-known coherent potential approximation (CPA), the appropriate conductance γ characterizing the disordered system is identified with the root of a self-consistent equation[37–41]

$$\left\langle \frac{\gamma_i - \gamma}{\gamma_i + (d-1)\gamma} \right\rangle = 0 \tag{A1}$$

in which angular brackets denote averages over the conductance distribution $\rho_L(\gamma_i)$, and d is the dimensionality of the lattice (i.e., the embedding dimension of the original disordered system).

Thus our algorithm for calculating the mobility of energetically and topologically disordered systems is the following: (1) Generate a cubic region of volume L^d containing a random distribution of sites, choosing the number of sites N_i in the region from the Poisson distribution $P(N) = e^{-\langle N\rangle} \times \langle N\rangle^N / N!$ appropriate to randomly distributed particles with mean density $n_0 = \langle N\rangle / L^d$; (2) Choose the energy of each site in the volume at random from the site energy distribution function $g(\epsilon_n)$ characterizing the model of interest; (3) Calculate the conductance of this region for a given bulk carrier concentration (which we do using a numerically exact supercell procedure summarized below); (4) Repeat this procedure for a sufficiently large number N_s of cubes, each one representing a randomly chosen cubic region of the actual disordered system, thereby accumulating a sample of conductances $\{\gamma_i\}$ representative of the distribution function $\rho_L(\gamma_i)$; (5) Numerically find the root of Eq. (A1) associated with the average of this conductance distribution, i.e., numerically obtain the root γ of the equation

$$\sum_{i=1}^{N_s} \frac{\gamma_i - \gamma}{\gamma_i + (d-1)\gamma} = 0. \tag{A2}$$

As shown previously,[25] the chief practical advantage of this procedure over a *direct average* of the block conductivity is that the ''effective medium average'' associated with Eqs. (A1) and (A2) is much less sensitive to the actual size of the cubes employed in the renormalization, thereby accelerating convergence to the infinite-system limit.

To implement this scheme requires a means for computing the conductance γ_i of each cube. In the present paper this

is formally done as described in Ref. 25, making use of the exact analysis in Ref. 26, which solves the problem of determining the conductance associated with a particular cubic region having N_i specifically located sites with specific randomly chosen energies. This is accomplished by replacing that part of the solid surrounding the cube of interest with identical copies of itself, infinite in number, identifying the diffusion tensor of each cube with that of an infinite system that is periodically repeated from the original one in all directions.[26] In Ref. 26 an exact relation for the diffusion tensor D for such a periodically-repeated system was obtained in terms of the eigenvalues and eigenstates of an associated $N_i \times N_i$ transition matrix. Although the analysis of Ref. 26 focused on the specific problem in which all transport sites are constrained to lie on an ordered lattice, the actual derivation and resulting relations for the diffusion constant do not actually make use of this property, and are valid for an initial cube containing arbitrarily-placed sites. The spectral relation derived in Ref. 26 is straightforward to numerically implement for cubes containing up to several hundred sites, as in the calculations presented in Secs. II–IV.

In addition to the diffusion tensor, computation of the equilibrium (i.e., low field) conductance of any such cube also requires the local carrier concentration x_i. This is obtained by first determining the chemical potential $\hat{\mu}$ which, through the equilibrium distribution $\rho(\epsilon)$ and site energy distribution function $g(\epsilon)$, determine the bulk carrier concentration $x = \int d\epsilon \ \rho(\epsilon) g(\epsilon)$ of the material. We assume noninteracting carriers described by an equilibrium site distribution function $\rho(\epsilon) = \exp[-\beta(\epsilon - \hat{\mu})]$. With $\hat{\mu}$ fixed, the local carrier concentration $x_i = \Sigma_{s=1}^{N_i} \rho(\epsilon_s)$ associated with the ith cube is then easily computed. Thus, using the local components of the diffusion tensor, calculated as described above, and the local carrier concentration we can compute the components of a cube conductance $\gamma_i = \gamma_0 x_i D_i$, where $\gamma_0 = e^2/kT$ is the usual combination of factors which relate the diffusion constant to the mobility. By computing this conductance for a sufficiently large number of randomly generated cubes we produce a reasonable sampling of the distribution $\rho_L(\gamma_i)$ of cube conductances, which can then be used in conjunction with Eq. (A2) to compute the bulk conductivity, which at fixed carrier concentration is simply proportional to the bulk mobility $\mu = \sigma/xe$. In all calculations appearing above for randomly distributed transport sites, the effective medium average for each macroscopic conductance was performed using a sample of $N_s = 300$ cube conductances γ_i, each one resulting from a solution to the eigenvalue equation for a randomly generated cube having an edge length L large enough to contain on average $\langle N \rangle = 100$ sites. These values were found to provide smooth statistically reproducible curves for computed mobilities as a function of mean interparticle separation $\rho = n_0^{-1/3}$. For the lattice calculations in Sec. IV, $N_s = 300$ cubic sections of a topologically ordered lattice, each section containing $N = 125 = 5 \times 5 \times 5$ sites and having an edge length $L = 5\rho$ were used to compute the block conductivities.

[1] L. B. Schein, Philos. Mag. B **65**, 795 (1992).
[2] P. M. Borsenberger and D. S. Weiss, *Organic Photoreceptors for Imaging Systems* (Marcel Dekker, New York, 1993); P. M. Borsenberger, E. H. Magin, M. van der Auweraer, and F. C. de Schryver, Phys. Status Solidi A **140**, 9 (1993).
[3] H. Bässler, Phys. Status Solidi B **175**, 15 (1993), and references therein.
[4] P. M. Borsenberger, L. Pautmeier, and H. Bässlr, J. Chem. Phys. **94**, 5447 (1991); P. M. Borsenberger, L. Pautmeier, R. Richert, and H. Bässler, *ibid.* **94**, 8276 (1991).
[5] B. Hartenstein, H. Bässler, S. Heun, P. Borsenberger, M. Van der Auweraer, and F. C. de Schryver, Chem. Phys. **191**, 321 (1995).
[6] Yu. N. Gartstein and E. M. Conwell, J. Chem. Phys. **100**, 9175 (1994); **217**, 41 (1994).
[7] T. Sasakawa, T. Ikeda, and S. Tazuke, J. Appl. Phys. **65**, 2750 (1989).
[8] Y. Kanemitsu and J. Einami, Appl. Phys. Lett. **57**, 673 (1990).
[9] H. J. Yuh and D. M. Pai, Philos. Mag. Lett. **62**, 61 (1990); Mol. Cryst. Liq. Cryst. **183**, 217 (1990); J. Imaging Sci. Technol. **36**, 477 (1992).
[10] T. Sugiuchi and H. Nishizawa, J. Imaging Sci. Technol. **37**, 245 (1993).
[11] A. Dieckmann, H. Bässler, and P. M. Borsenberger, J. Chem. Phys. **99**, 8136 (1993); P. M. Borsenberger and J. J. Fitzgerald, J. Phys. Chem. **97**, 4815 (1993); M. B. O'Regan, P. M. Borsenberger, and W. T. Gruenbaum, Phys. Status Solidi **148**, 259 (1995).
[12] S. V. Novikov and A. V. Vannikov, JETP **79**, 482 (1994).
[13] R. H. Young and J. J. Fitzgerald, J. Chem. Phys. **102**, 2209 (1995).
[14] S. V. Novikov and A. V. Vannikov, J. Phys. Chem. **99**, 14573 (1995).
[15] Yu. N. Gartstein and E. M. Conwell, Chem. Phys. Lett. **245**, 351 (1995).
[16] R. H. Young, Philos. Mag. B **72**, 435 (1995).
[17] D. H. Dunlap, P. E. Parris, and V. M. Kenkre, Phys. Rev. Lett. **77**, 542 (1996).
[18] S. V. Novikov and A. V. Vannikov, Proc. SPIE **2850**, 130 (1996).
[19] P. E. Parris, Proc. SPIE **2850**, 139 (1996).
[20] D. H. Dunlap, Proc. SPIE **2850**, 110 (1996).
[21] L. Th. Pautmeier, J. C. Scott, and L. B. Schein, Chem. Phys. Lett. **197**, 6 (1992).
[22] J. W. Stasiak, T. J. Storch, and E. Mao, Proc. SPIE **2526**, 23 (1995).
[23] J. Veres and C. Juhasz, Philos. Mag. B **75**, 377 (1997).
[24] U. Wolf, H. Bässler, P. M. Borsenberger, and W. T. Gruenbaum, Chem. Phys. (in press).
[25] B. D. Bookout and P. E. Parris, Phys. Rev. B **48**, 12637 (1993).
[26] P. E. Parris and B. D. Bookout, Phys. Rev. Lett. **71**, 16 (1993).
[27] A. Miller and E. Abrahams, Phys. Rev. **120**, 745 (1960).
[28] G. Schoenherr, H. Bässler, and M. Silver, J. Phys. Colloq. **4**, 42 (1981).
[29] V. Ambegaokar, B. I. Halperin, and J. S. Langer, Phys. Rev. B **4**, 2612 (1971).
[30] N. F. Mott, Philos. Mag. **19**, 835 (1969).
[31] N. Apsley and H. P. Hughes, Philos. Mag. **30**, 963 (1974).
[32] D. H. Dunlap and V. M. Kenkre, Chem. Phys. **67**, 178 (1993); V. M. Kenkre and D. H. Dunlap, Philos. Mag. **65**, 831 (1992).
[33] D. M. Pai, J. Chem. Phys. **52**, 2285 (1970).
[34] W. D. Gill, J. Appl. Phys. **43**, 5033 (1972).
[35] D. Stauffer, in *Introduction to Percolation Theory* (Taylor & Francis, London 1985), pp. 70–89.
[36] B. D. Hughes, in *The Mathematics and Physics of Disordered Media*, edited by B. D. Hughes and B. W. Ninham (Springer, Berlin, 1983).
[37] S. Kirkpatrick, Rev. Mod. Phys. **45**, 574 (1973); M. Sahimi, B. D. Hughes, L. E. Scriven, and H. T. Davis, J. Chem. Phys. **78**, 6849 (1983).
[38] H. D. Huber, Phys. Rev. B **20**, 5333 (1979); in *Excitation Dynamics in Molecular Solids*, Vol. 49 in *Topics in Applied Physics*, edited by W. M. Yen and P. M. Selzer (Springer, Berlin, 1981).
[39] S. Alexander, J. Bernasconi, W. R. Schneider, and R. Orbach, Rev. Mod. Phys. **53**, 175 (1981).
[40] T. Odagaki and M. Lax, Phys. Rev. B **25**, 2301 (1982); **24**, 5284 (1981); T. Odagaki, M. Lax, and A. Puri, *ibid.* **28**, 2755 (1983).
[41] P. E. Parris, Phys. Rev. B **36**, 5437 (1987).